Seismic retrofit of RC building structures with Buckling Restrained Braces

André Almeida, Ricardo Ferreira *, Jorge M. Proença, António S. Gago

CERIS, Instituto Superior Técnico, Universidade de Lisboa, Av. Rovisco Pais 1, 1049-001 Lisboa, Portugal

ABSTRACT

The search for passive control systems has increased in some high seismicity areas of the world, especially in terms of the strengthening of existing RC or steel building structures designed without earthquake-resistance considerations (pre-code structures) or with outdated structural codes. One of the most promising techniques consists of adding steel Buckling Restrained Braces (BRBs) to the existing structure. This paper presents an applicability study of these devices in the retrofit of a typical existing RC pre-code school building structure. The effectiveness of the retrofit solution, initially designed according to Kasai et al. (1998) formulation, was assessed through non-linear static and dynamic numerical analyses. The results of these analyses, led to the design method being developed with the purpose of optimising the dimensions of the steel dampers at different storeys and therefore improving the structural performance. This development is based on a simplified method of predicting the response of a passive system, by devising a single degree of freedom system. The effectiveness of the seismic retrofit solution designed through the improved design procedure was confirmed, showing that the studied strengthening solution results in a significant increase in strength, deformation and energy dissipation capacity, thereby limiting damage in the original structure to admissible levels.

© 2016 Elsevier Ltd. All rights reserved.

1. Introduction

For the past four decades, the research on modern technology for seismic damage mitigation, such as base isolation and other passive control systems has been a major issue around the world, notably in Japan. After the 1995 Hyogo-Ken Nanbu earthquake, which led to numerous building collapses and costly structural repairs in the city of Kobe, modern seismic protection systems quickly grew to replace conventional structural solutions. The pursuit of innovative seismic protection solutions and their acceptance has also increased in other high seismicity countries and regions such as the USA and Italy.

The awareness of the consequences of major seismic events around the world has resulted in a growing concern about the structural safety of both new and old structures. Given the impossibility of analysing and intervening on all the structures simultaneously, it is essential to establish priorities for large-scale seismic assessment and retrofitting. In this context, public buildings (such as state school buildings) assume a particular importance.

The need to update the school building stock of state secondary schools in mainland Portugal led to the creation of state-run enterprise named Parque Escolar. One of its functions is to assess the level of structural safety of existing school buildings, their compliance with current building codes and the need for retrofit interventions. One of the schools chosen for structural retrofitting is presented as a case study in this paper. The school, Escola Secundária Poeta António Aleixo, is in Portimão, which is a city with one of the highest seismicity levels in mainland Portugal (actual reference return period of 475 years, peak ground acceleration on type A, rock or rock-like, ground of 2.5 m/s^2) [1]. The school structure was designed in the mid-1950s, prior to the enforcement of the first Portuguese seismic design code (1958).

1.1. Buckling Restrained Braces

Buckling Restrained Braces (BRBs) have proved to be beneficial in providing resistance against horizontal earthquake ground motions while simultaneously enhancing the energy dissipation capacity of both new and existing steel structures. However, their applicability and effectiveness in RC framed structures is still uncertain. A relatively large number of different types of BRBs have been studied, tested and proposed in the past few decades. Regardless of detailing differences, they all share the same concept: to

---

* Corresponding author.
  E-mail address: ricardo.a.ferreira@ist.utl.pt (R. Ferreira).

prevent both global and local (cross-section) buckling in the braces and allow equal tensile and compressive strength, and thus higher hysteretic energy dissipation.

The use of BRBs overcomes the typical disadvantages of normal braces, i.e. the asymmetrical hysteretic behaviour in tension and compression and the substantial strength deterioration when cyclically loaded.

The most common configuration of a BRB (Fig. 1) consists in a steel profile encased in a circular or rectangular hollow section steel profile, filled with concrete or mortar. The main purpose of the concrete-filled tube is to prevent the buckling of the steel core (that entirely sustains the axial force). The steel core-concrete interface usually consists of a slip surface to allow relative axial deformations between the steel core and the tube infill. The slip surface is achieved by placing a low friction material between the infill material and the steel core. The transversal expansion of the brace under compressive loads due to Poisson's effect should be accommodated providing a gap between the brace and the encasing material. In addition, the dissipative part of the brace, which is the zone where yielding occurs, can be replaced by detaching it from the brace non-yielding segment, which is retained (e.g., in the aftermath of a major seismic event).

1.2. Codes and regulations

In Japan, BRBs are regarded as dampers and, therefore, are regarded as a type of passive control system or scheme for seismic damage mitigation [2].

According to Kasai [3], BRBs became a viable means of enhancing the seismic performance of buildings with the publication of the JSCA Specifications in December 2000 and the publication of the JSSI Manual in October 2003. More than fifty university researchers, structural designers and engineers from about twenty damper manufacturing companies were involved in developing the JSSI Manual. It refers to the various aspects of passive control schemes, such as the damper mechanism, design, fabrication, testing, quality control and analytical modelling, as well as the analysis, design and construction of passively controlled buildings.

In the USA, BRBs have been code regulated since the release of NEHRP Recommended Provisions for Seismic Regulations for New Buildings and Other Structures (FEMA 450-1) in 2003 [4]. This document provides specific rules for BRBs and other structural elements of steel BRB frames, as well as qualifying cyclic tests. As mentioned in [4], the document's recommendations for BRBs should be used in conjunction with AISC Seismic Provisions for Structural Steel Buildings [5], even though this version of AISC Seismic Provisions did not include any specific provisions regarding BRBs. It was not until 2005 that AISC Seismic incorporated, in a later version, provisions for the use of BRBs in steel buildings [6]. However, at the time, no provisions were issued for BRBs in composite steel concrete or reinforced concrete buildings. In Europe, seismic design codes omit the design of BRBs. However, despite omitting design and detailing provisions, some codes allow for the use of such devices in seismic protection. In Italy, the most recent normative environment is embodied in the NTC'08 [7], comparable to the former OPCM3431/05 [8] and in its predecessor OPCM3274/03 [9]. The NTC'08 allows for the use of anti-seismic dissipative devices (e.g., braces) in both new and existing structures, setting forth general design rules and providing for other relevant indications (e.g., compliance tests and installation, maintenance and replacement related requirements). Moreover, in 2009 the European Committee for Standardisation (CEN) issued the European Standard EN15129 [10], which contains provisions for performance requirements, materials and testing of displacement dependent devices, besides other seismic devices such as velocity dependent devices and isolators.
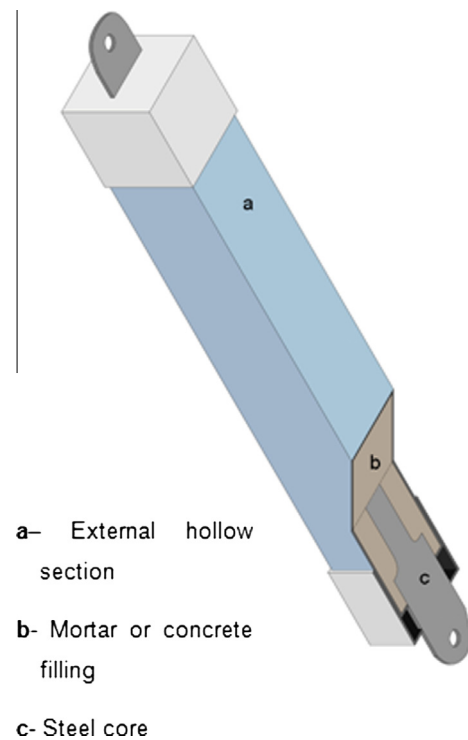

a– External hollow section

b- Mortar or concrete filling

c- Steel core

Fig. 1. Traditional BRB configuration.

As a preliminary conclusion one could state that the use of BRBs for new steel buildings is reasonably framed by codes and regulations, contrarily to what happens in their use in reinforced concrete (or composite) buildings. This remark becomes even more critical in the retrofit of old, pre-code or low-code, reinforced concrete buildings, where the stable energy-dissipation capabilities of BRBs could provide for a promising retrofitting solution (as long as the specificities of these structures, such as low ductility and deformation capacity, are properly considered).

2. Review of BRB design procedure

Given the nonlinear nature of its dynamic behaviour, the BRB design should be based on nonlinear dynamic analysis. On the other hand, the absence of specific design provisions for BRB use in retrofitting RC structures indicates that known preliminary design methods, should be adopted, such as those used for hysteretic steel dampers in steel frames (henceforth simply referred to as dampers). For the purpose of our work, the design method formulated by Kasai et al. [11] was used. This method is based on devising a single degree of freedom (SDOF) system that has the same vibration period as the multiple degree of freedom (MDOF) of the structure under assessment.

With the exception of the BRBs, which are assumed to have elastoplastic behaviour, the existing structure should remain in the elastic domain for the whole duration of the seismic ground motion. The objective of this premise is that all potential seismic damage (plastic deformations) is concentrated in the BRBs.

Fig. 2 illustrates the SDOF model devised for a structure with added hysteretic damper elements. This model is composed of two sets of springs in parallel, together with another spring placed in series, connected to a mass M. The set consisting of two springs placed in series is called sub-system "a". Sub-system "a" represents the brace-damper assembly added to the framed structure, in which K_b is the brace non-yielding segment (non-dissipative part of the BRB) stiffness, K_d is the damper (dissipative part of the
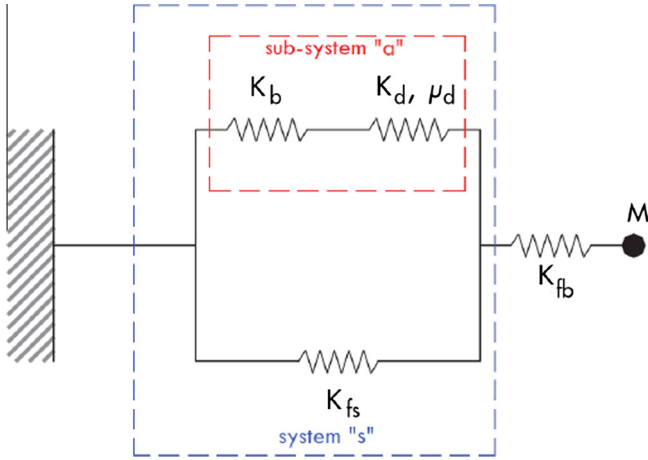
Fig. 2. SDOF model (adapted from Castellano et al. [12]).

BRB in this study) elastic stiffness and μ_d is the damper ductility demand, that is the ratio between ultimate and yield horizontal deformations of the steel damper. In parallel to sub-system "a" there is a set composed of a single spring representing the shear stiffness of the original frame, K_{fs}. The spring (K_{fb}), placed in series with the other sets, represents the bending stiffness of the frame. Since the horizontal displacements, caused by global frame flexure are expected to be negligible (particularly in low-rise RC buildings, due to the high axial stiffness presented by the vertical structural elements), K_{fb} can be taken as infinite. The whole set formed by the added brace-damper assembly and the original frame in shear is called system "s".

BRBs design should aim for the largest response reduction, in terms of both of displacement and acceleration, which can be expressed by means of the peak response of the damped system. For this, the equivalent vibration period T_{eq} and the equivalent damping ratio ξ_{eq} should be computed. T_{eq} depends on the vibration period of the original framed structure in shear T_{fs}, its shear stiffness K_{fs} and the equivalent stiffness K_{eq} Eq. (1).

$$T_{eq} = T_{fs} \times \sqrt{\frac{K_{fs}}{K_{eq}}} \tag{1}$$

Then, K_{eq}, represented in Fig. 3, can be determined through Eq. (2), with p given by Eq. (3). If $K_b = \infty$, μ can simply be assumed to be same as μ_d. For the purpose of this work, μ_d has been assumed to be 7.

$$K_{eq} = \frac{1 + p \times (\mu - 1)}{\mu} \times K_s \tag{2}$$

$$p = \frac{K_{fs}}{K_s} \tag{3}$$

ξ_{eq} is evaluated through Eq. (4), where ξ_f is the damping ratio of the original framed structure.

$$\begin{aligned}\xi_{eq} &= \xi_f + \frac{1}{\mu} \int_1^\mu \frac{2(1-p)(\mu'-1)}{\pi\mu'(1+p(\mu'-1))} d\mu' \\ &= \xi_f + \frac{2}{\pi \times p \times \mu} \times \ln\left(\frac{1+p(\mu-1)}{\mu^p}\right) = \xi_f + \Delta\xi\end{aligned} \tag{4}$$

Eq. (4) shows that the equivalent damping ratio is increased from that of the original framed structure through a coefficient ($\Delta\xi$) that depends on the average of the hysteretic damping ratio, with ductility demand μ' varying from 1 (no plasticity) to peak ductility demand μ. The expression inside the integral derives from the consideration that hysteretic damping ratio ξ_0 can be calculated as the

energy dissipated per cycle divided by 4π times the elastic strain energy obtained from the secant stiffness. Knowing the equivalent period and damping ratio, we can estimate the peak response of the SDOF passive system, both in terms of displacement S_d and acceleration S_{pa}. The peak response can be obtained from a common linear response spectrum using T_{eq} and ξ_{eq}.

The response reduction is computed as the ratio of peak responses of system "s" to those of the original structure (determined with T_{fs}, ξ_f and also considering a linear response spectrum), as expressed in Eqs. (5) and (6) where S_{pa} and S_d are pseudo-acceleration and displacement spectral values, respectively.

$$R_{pa} = \frac{S_{pa}(T_{eq}, \xi_{eq})}{S_{pa}(T_{fs}, \xi_f)} \tag{5}$$

$$R_d = \frac{S_d(T_{eq}, \xi_{eq})}{S_d(T_{fs}, \xi_f)} \tag{6}$$

The inclusion of dampers in structures has two effects: it decreases of the vibration period from T_{fs} to T_{eq}, because of structural stiffening, and it increases the hysteretic damping from ξ_f to ξ_{eq}. Based on the consideration of these two effects, the reduction factors can be expressed differently, making use of a damping factor D_ξ, as follows:

$$R_{pa} = \frac{S_{pv}(T_{eq}, \xi_f)}{S_{pv}(T_{fs}, \xi_f)} \times \frac{T_{fs}}{T_{eq}} \times D_\xi \tag{7}$$

$$R_d = \frac{S_{pv}(T_{eq}, \xi_f)}{S_{pv}(T_{fs}, \xi_f)} \times \frac{T_{eq}}{T_{fs}} \times D_\xi \tag{8}$$

S_{pv} represents the pseudo velocity spectrum, while the damper factor D_ξ accounts for the hysteretic damping increase and was derived statistically from ensemble group of 31 earthquakes observed over vibration periods ranging from 0.2 to 3 s [13], and representing an average reduction of S_d, S_{pv} and S_{pa}. The proposed formula for the evaluation of D_ξ is as follows:

$$D_\xi = \sqrt{\frac{1 + 25 \times \xi_f}{1 + 25 \times \xi_{eq}}} \tag{9}$$

Assuming that peak acceleration in hysteretic passively controlled systems with elastoplastic dampers peak acceleration is synchronised approximately with peak (relative) displacement, then peak acceleration or base shear reduction R_a can be taken as:

$$R_a = R_{pa} \tag{10}$$

The choice of damper elastic stiffness should be based on the response reduction estimations. Naturally, it depends on the objectives and desired performance. Fig. 4 shows a typical example of an R_a vs R_d plot, where each point represents a different value of K_d. Once the value of K_d has been set, it is necessary to convert the SDOF system into a multiple degree of freedom (MDOF) system, that is to say, one that determines the total damper stiffness at each storey. Simplified closed-form formulae ((11) and (12)) can be used for this. The formulae are based on the following constraints:

(1) The ratio of damper strain energy to total system strain energy for the MDOF passive system becomes the same as that of the SDOF passive system;
(2) Under the design shear force, distributions of drift angle and ductility demand of the MDOF passive system are uniform, whilst those of the frame without dampers may be non-uniform;
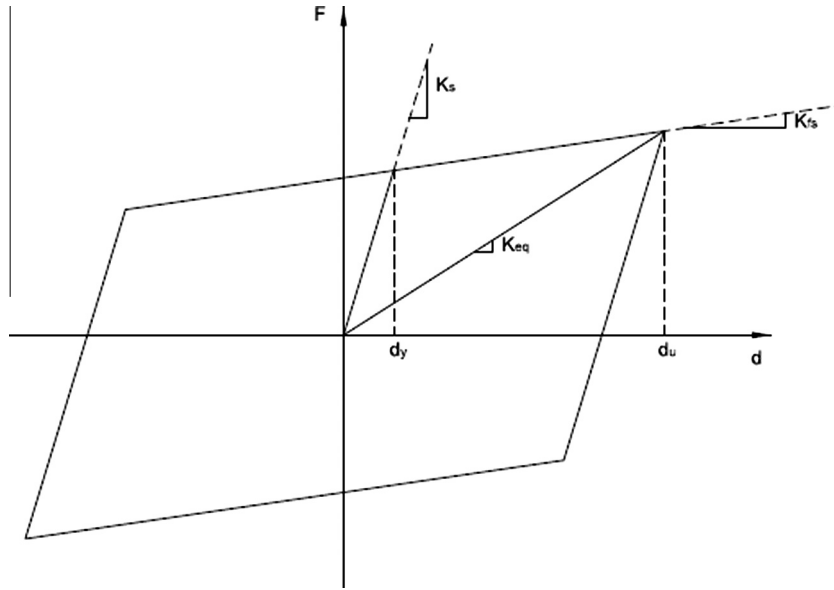(3) The elastic vibration period of the MDOF passive system becomes the same as that of the SDOF passive system.

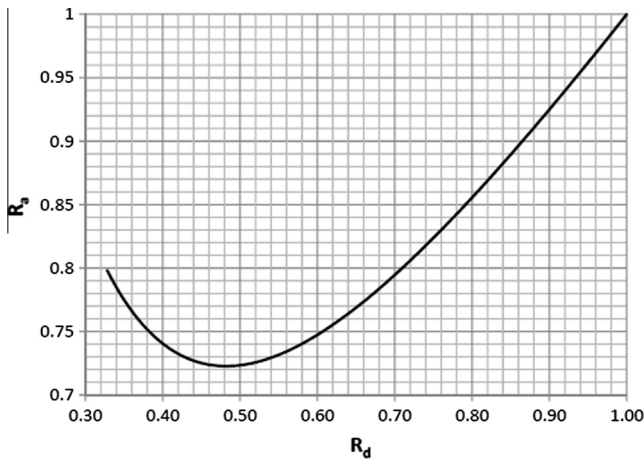**Fig. 3.** Cyclic force-displacement relation conceived for SDOF system and equivalent secant stiffness.

Fig. 4. Example of R_a-R_d plot.

Assuming that both storey height and weight are constant along the building height, identical damper-brace non-yielding segment assemblies at storey i and $K_d = \infty$, constraints 1 and 2 lead to Eqs. (11) and (12).

$$\frac{K_d}{K_d + K_{fs}} = \frac{\sum K_{d,i}}{\sum (K_{d,i} + K_{fs,i})} \tag{11}$$

$$\frac{V_i}{K_{d,i} + K_{fs,i}} = \frac{\sum V_i}{\sum (K_{d,i} + K_{fs,i})} \tag{12}$$

In these expressions, V_i, $K_{fs,i}$ and $K_{d,i}$ are, respectively, the shear force, the shear stiffness of the frame and the damper horizontal elastic stiffness at storey i. Eq. (13) derives from Eqs. (11) and (12), allowing the determination of damper horizontal stiffness at each storey.

$$K_{d,i} = \left(\frac{V_i}{K_{fs,i}} \times \frac{\sum K_{fs,i}}{\sum V_i} \times \left(1 + \frac{K_d}{K_{fs}} \right) - 1 \right) \times K_{fs,i} \tag{13}$$

Finally, the evaluation of the yield forces is necessary so as the complete preliminary design of the damper. Assuming that base shear at peak ductility demand in the controlled system is (14):

$$R_a \times V_f \tag{14}$$

where V_f is the elastic peak base shear of the framed structure, the yielding base shear F_y of the damper can be determined through Eq. (15):

$$R_a \times V_f = F_y + K_{fs} d_y (\mu - 1) \tag{15}$$

Taking into account Eqs. (3) and (15) can be rewritten as:

$$F_y = \frac{R_a \times V_f}{1 + p \times (\mu - 1)} \tag{16}$$

The portion of F_y that is taken up by the damper at storey i is determined by considering the ratio of damper stiffness to total stiffness at storey i, as expressed in Eq. (17), where once again $K_{b,i}$ is taken as infinite.

$$F_{yd,i} = \frac{R_a \times V_i}{1 + p_1 \times (\mu - 1)} \times \frac{K_{d,i}}{K_{d,i} + K_{fs,i}} \tag{17}$$

Considering that in this case the hysteretic dampers are BRBs, the elastic axial stiffness of each BRB is obtained by dividing the values given by Eq. (13) by the number of BRBs per storey and by $\cos^2 \beta_i$, being β_i the inclination angle of the BRB at storey i. Analogous reasoning should be followed for the computation of the axial yield force of each BRB, dividing by $\cos \beta_i$ instead.

The former design procedure was devised for steel frames fitted with BRBs. The extension to other structural types, namely RC frame buildings (either new or to be retrofitted) needs to be clarified. Some of the hypotheses underlying the design procedure may not be valid in this extension. The assumption that the original structure remains in the linear range conflicts with the highly nonlinear behaviour presented by concrete, even for small strains. Similarly, the assumption that, under the design shear force, the drift angles in a structure with added dampers are constant along the building height may be unrealistic, particularly in the case where the distribution of drift angles in the original structure is non-uniform. Although a uniform drift distribution prior to the yielding of dampers can be achieved through an accurate choice of damper elastic stiffness, after that, the structural response might be governed by the original structure. Moreover, the reduced deformation capacity of old RC building structures may pose some limitations and lead to a revision of the presented design procedure.

All these uncertainties were further clarified by the detailed study presented in the following chapters corresponding to a typical low-code (or no-code) RC frame building.

3. Case study presentation

The case study consists of a three-storey school building with a rectangular floor plan, with approximate dimensions of 40×17 m, representing (which fits has consistent representative of) the buildings that comprise the school complex under study. The layout conforms to the architectural central corridor model with two lateral rows of classrooms. Four longitudinal nine-bayed frames, two for the façades and two for the corridor, comprise the RC structure. There are also two transversal frames at the extremities. The classroom floors consist of transversely oriented ribbed slabs, whereas the corridor consists of a solid slab. The columns foundations are usually square or rectangular superficial RC footings. Smooth steel rebars were used in all structural elements.

The analysis of the design documentation led to the following conclusions: (i) these school buildings were not designed for seismic loads; (ii) the columns were designed on the assumption that they would be subjected only to pure centred axial compression. The detailing and design methods originally considered suggest reduced resistance and deformation capacity under lateral loads of the loadbearing vertical elements.

In this study the seismic assessment of the existing and retrofitted building was conducted through a nonlinear analytical model developed using *SeismoStruct* software [14]. All beam-column joints were assumed to be monolithic, while the columns were considered to be pinned at their base due to poor reinforcement of the column-footing joints. The inelastic behaviour of the RC elements was established at cross-section level, with nonlinear models being used for each of the materials i.e. reinforcing steel and concrete (core and cover). With respect to the nonlinear behaviour of concrete, the constitutive relation proposed by Mander et al. [15] and revised under the rules for cyclic degradation proposed by Martínez-Rueda and Elnashai [16], was adopted. Mander et al. [15] proposed a unified stress-strain approach for confined concrete with monotonic loading at slow strain rates, applicable to both circular and rectangular transverse reinforcement. Apart from the influence of the confinement of concrete provided by ties and stirrups, only the uniaxial behaviour of materials was modelled.

The model adopted for the nonlinear behaviour of reinforcing steel uses the stress-strain relation proposed by Menegotto and Pinto [17], together with an isotropic hardening rule proposed by Filippou et al. [18] and the post-elastic buckling rules proposed by Monti and Nuti [19]. This model features an additional memory rule proposed by Fragiadakis et al. [20] that ensures greater numerical stability and accuracy under transient seismic loading, calibrated for smooth reinforcing bars [21].

4. Pushover analysis results

A static pushover analysis was performed with a nonlinear model, featuring BRBs placed in all bays of both facades in a chevron configuration (Fig. 5).

The pushover analyses were performed incrementally under force control, considering a lateral load pattern based on the product of the fundamental mode shape displacements at storey levels by the corresponding masses. These analyses were preceded by the application of the vertical loads (dead and fraction of the live loads). The computation of the performance point was achieved using the capacity spectrum method, as presented in ATC 40 [22].

Only the results of BRB design for the longitudinal direction analysis are presented. The incremental lateral forces were applied as shown in Fig. 5.

The mechanical characteristics of the BRBs designed as previously described are presented in Table 1, while the corresponding dimensions are shown in Table 2.

In an initial stage, the structural retrofitting solution featured only BRBs placed in the corner bays of the building. However, this configuration had to be discarded due to the significantly high uplift forces imposed in adjacent columns and foundations. Hence, the number of BRB was successively increased until the uplift forces were within acceptable values, leading to BRBs in all peripheral bays. Furthermore (and despite not having been checked) the spatial dissemination of the BRBs is favourable to the horizontal compatibility forces that have to be transmitted though the slab and beam structural elements.

The constitutive relationships for BRBs yielding (dissipative) segments were based in the Menegotto-Pinto steel model with Monti-Nuti post-elastic buckling (and modifications introduced by Fragiadakis), as included in Seismostruct [14]. The slenderness ratio, L/Φ, which determines the (in this case limited) extent of buckling was taken as 5 (L and Φ are, respectively, the longitudinal distance between equivalent intermediate supports preventing lateral deflection and the cross-section dimension).

Fig. 6 presents the capacity curves obtained through pushover analysis conducted on the models of the original structure with and without BRBs.

The red[1] $\times$ marker represents the performance point, determined by the capacity spectrum method described in [22], considering the elastic response spectrum prescribed in NP EN 1998-1 [1] with a spectral acceleration value of 3.9 m/s^2 for null periods, corresponding to a return period of 821 years (importance class III). The performance point corresponds to a top storey displacement $\Delta = 12.8$ cm and base shear $F_b = 3926.7$ kN. Since the third storey is 10.6 m above ground, a top storey displacement of $\Delta = 12.8$ cm corresponds to a global drift angle $\theta = 0.0121$ rad.

This value meets the structural performance level designated by Damage Control in [22], which is considered to be satisfactory. However, after early yielding of the BRBs, the drifts become non-uniform, with deformations mainly concentrated in the most flexible storey, which in the present case is the first one (where columns are pinned at their base). Naturally, this results in exceptionally high ductility demands μ for the BRBs of the first storey, as shown in Table 3.

Table 4 presents the relative horizontal displacements d_r and the corresponding drift angle θ at the performance point (top storey). Although the drift angles of second and third storeys are very small, the first storey drift is unacceptable according to the standards in [22].

The significantly low capacity curve of the original structure is a consequence of the lack of seismic design provisions in the standards applicable at the time of construction (leading to abnormally low values of both lateral stiffness and strength). More specifically and concurrently, the use of limited capacity materials (particularly concrete) and outdated design and detailing rules – the columns were designed for pure axial compression, considered pinned at their base, with large stirrup spacing and insufficient anchorage of the rebars at the beam-column joints –which also serves as justification for the characteristics of the capacity curve.

---

[1] For interpretation of color in Fig. 6, the reader is referred to the web version of this article.
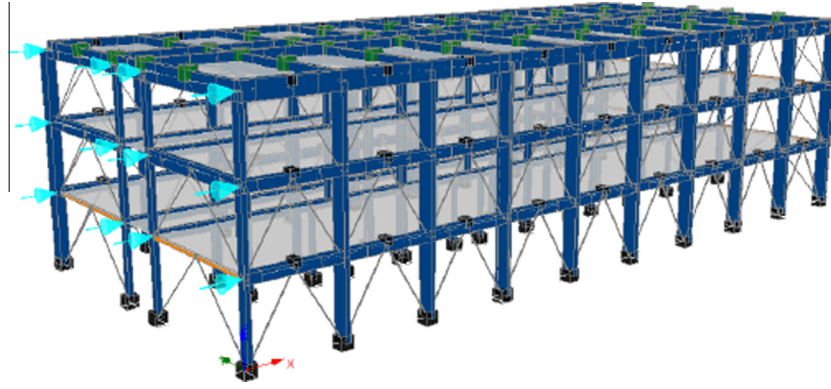
Fig. 5. Numerical model.

Table 1
Total horizontal BRB stiffness and yield force at each storey.

Storey	K_d (kN/m)	F_{yd} (kN)
1	719,023	3394
2	535,333	2506
3	244,574	1125

Table 2
Cross-section area and length for each BRB at different storeys.

Storey	A (cm^2)	L (m)
1	5.05	1.40
2	3.66	1.41
3	1.64	1.39

Fig. 6. Capacity curves of original structure and structure retrofitted with BRBs.

Table 3
Ductility demands for BRBs at each storey.

Storey	μ
1	16.01
2	2.05
3	2.23

Table 4
Storey drift, heights and drift angles.

Storey	d_r (m)	h (m)	θ (rad)
1	0.099	3.6	0.0274
2	0.014	3.5	0.0040
3	0.015	3.5	0.0044

5. Revision of design procedure

In order to overcome the non-uniformity of storey drift, which in our case results in damage concentrated in the first storey, an additional step in design procedure formulated by [11] is proposed.

Ideally, because yielding of BRBs in the most flexible storeys is delayed, drifts should become uniform at the performance point. The yielding of BRBs in storey i can be delayed by using an overshoot factor γ_I for the yield strength of the BRB. The computation of γ_i is based on the assumption that the force-displacement relation in each storey is bilinear, as in [11]. Accordingly, the relative displacement of storey i at the performance point, Δ_i, is given by Eq. (18), where $F_{y,i}$ and F_i are, respectively, the shear forces for yielding and performance points of storey i.

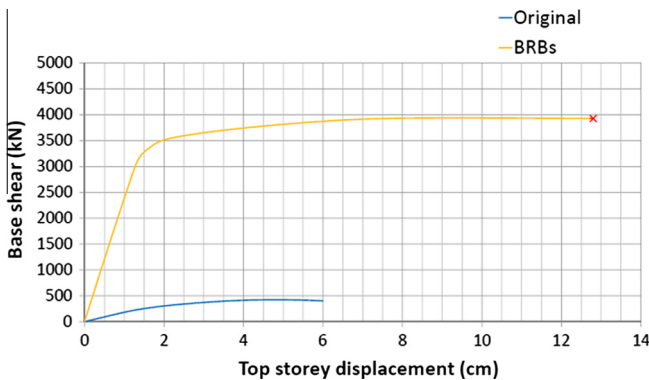$$\Delta_i = \frac{F_{y,i}}{K_{s,i}} + \frac{F_i - F_{y,i}}{K_{fs,i}} \tag{18}$$

The overshoot factor γ_i can be determined by imposing equality between the modified drift of storey i, $\Delta_i(\gamma_i)$, and the desired drift value Δ_d. The performance point $\Delta_i(\gamma_i)$ is given by Eq. (19), similar to Eq. (18), accounting for the increase of BRB yield strength $F_{yd,i}$. The value of $F_{i,new}$, is given by Eq. (19).

As γ_i is obviously unknown, $F_{i,new}$ can only be determined by taking into consideration the shear force corresponding to Δ_d at a reference storey r and knowing the ratios between storey shear that correspond to a uniform distribution of drift.

Assuming an inertial force distribution proportional to the product of storey mass and to the corresponding displacement in the fundamental mode of vibration, the ratios between storey shear forces for a uniform distribution of storey drift become proportional to the product of storey mass and storey height above ground.

However, by defining C_{ir} as the ratio between the shear force at storeys i and r, assuming a uniform distribution of drifts, and assuming F_r the shear force corresponding to Δ_d at storey r, Eq. (19) can be rewritten with $C_{ir}F_r$ instead of $F_{i,new}$.

Taking Δ_d as the reference storey drift at the performance point given by Eq. (18) where index i = r, and equalising it to $\Delta_i(\gamma_i)$, γ_i, results in Eq. (21).

Since the ductility demands of BRBs in the second and third storeys were similar (see Table 3), we introduced a simplification. Deeming the drifts of these two storeys to be equal at the performance point, the overshoot factor γ was only computed for the yield strength of the first storey BRBs. The storey taken as reference was storey two. However, instead of second floor F_r, the base shear F_b was considered. Moreover, since $K_{d,1}/K_{s,1}$ = 0.96, for simplification purposes, $F_{yd,1}$ was considered to be equal to $F_{y,1}$. Thus, γ

was determined through Eq. (22), where base shear at the performance point is $F_b = F_1$.

$$\Delta_i(\gamma_i) = \frac{F_{y,i} + F_{yd,i}(\gamma_i - 1)}{K_{s,i}} + \frac{F_{i,new} - [F_{y,i} + F_{yd,i}(\gamma_i - 1)]}{K_{fs,i}} \qquad (19)$$

$$F_{i,new} = \left[\Delta_d - \frac{F_{y,i} + F_{yd,i}(\gamma_i - 1)}{K_{s,i}}\right] \times K_{fs,i} + F_{y,i} + F_{yd,i}(\gamma_i - 1) \qquad (20)$$

$$\gamma_i = \frac{1}{F_{yd,i}\left(\frac{1}{K_{s,i}} - \frac{1}{K_{fs,i}}\right)}$$
$$\times \left[\frac{F_r + F_{yr}(p_r - 1)}{K_{fs,r}} - \frac{F_{y,i} - F_{yd,i}}{K_{s,i}} - \frac{C_{ir}F_r - F_{y,i} + F_{yd,i}}{K_{fs,i}}\right] \qquad (21)$$

$$\gamma = \frac{\frac{K_{fs,i}}{K_{fs,2}}[C_{21}F_b + F_{y,2}(p_2 - 1)] - F_b}{F_{y,1}(p_1 - 1)} \qquad (22)$$

Considering F_b = 3926.7 kN, which resulted from the previous analysis, expression (22) gives γ = 1.078. Assuming that the increase of the first storey BRBs yield strength is equal to the increase of F_b (the increase of yield drift is small), an increased value of base shear at the performance point $\overline{F_b}$ can be estimated. Through Eq. (23), where $F_{yd,1}$ is the originally determined total horizontal yield force of first storey BRBs and using $\overline{F_b}$ in Eq. (21) instead of F_b, gives γ = 1.132.

$$\overline{F_b} = F_b + (F_{yd,1} \times \gamma - F_{yd,1}) \qquad (23)$$

Repeating the pushover analysis, taking the yield strength of first storey BRBs increased with $\overline{\gamma}$, a new capacity curve was determined (Fig. 7). As expected, for the same displacements the base shear increased in relation to the capacity curve shown in Fig. 6. The new performance point corresponds to a top storey displacement Δ = 12.2 cm (smaller than that previously obtained) and F_b = 4329.6 kN. As shown in Table 5, the ductility demands level out and become closer to μ_d = 7 considered in the design, and the interstorey drift results also became more uniform (as shown in Table 6), as the second and third storey drifts increased and the first storey drift decreased. In terms of performance, the drift values obtained meet the standards of Damage Control with a wide margin.

6. Nonlinear dynamic analysis results

Three artificial accelerograms, named A, B and C were generated according to Portuguese standard [1] (national version of Eurocode 8 [23], taking into account local seismicity studies). These artificial accelerograms were generated considering the provisions of Eurocode 8, namely those stated in clause 3.2.3.1.2, i.e., so as to match the elastic response spectrum given in clause 3.2.2.2 for 5% damping, and, in this specific study, importance class III, ground type C and type 1 earthquake. The duration of the accelerograms was approximately 40 s because the provision of the Portuguese National Annex of [1] specifies that the minimum duration of the stationary part should be 30 s. The artificial accelerograms were applied in the longitudinal direction only, in such a way as to allow for a more immediate comparison with the pushover analysis results.

Three analyses were considered, each with a different artificial accelerogram (A, B and C). The most unfavourable results drawn from the three analyses were taken as the action effects. According to [23], two conditions needed to be met by the chosen artificial accelerograms. The first condition is that the mean value of spectral acceleration for null periods should not be less than ag × S. In our case study, ag × S = 3.90 m/s², whereas the mean value of spectral acceleration for T = 0 s is S_a = 4.34 m/s², meaning that the
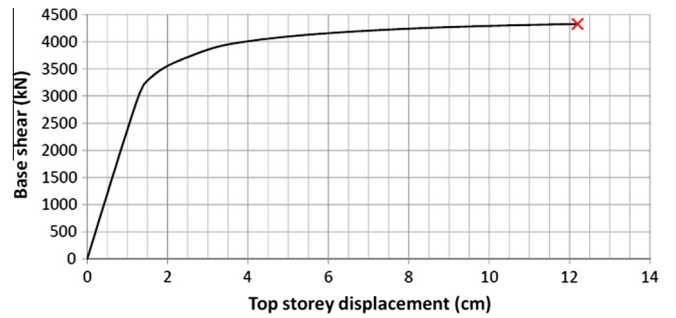

Fig. 7. New capacity curve.

Table 5
Ductility demands of BRBs at each storey.

Storey	μ
1	5.72
2	6.22
3	6.96

first condition is met. The second condition was that for period values ranging from $0.2T_1$ and $2T_1$, with T_1 being the period of the fundamental mode of vibration, no value of the mean response spectrum (resulting from the three artificial accelerograms) should be less than 90% of the corresponding value of the response spectrum provided by the code with 5% damping. In our case, T_1 = 0.364 s, thus:

$$\begin{cases} 0.2T_1 = 0.0728 \text{ s} \\ 2T_1 = 0.728 \text{ s} \end{cases}$$

The response spectra for the artificial accelerograms, the mean response spectrum and the elastic response spectrum of [1] reduced to 90%, are shown in Fig. 8.

Additionally, these dynamic analyses assumed an overshoot factor of γ = 1.132 for first storey BRB yield strength.

Fig. 9 shows overall peak and maximum residual interstorey drifts arising from the application of accelerograms A, B and C, at each storey. This figure shows that while accelerogram A caused the largest drifts in first and third storeys, the largest drifts in the second storey were caused by accelerogram B.

The performance levels were checked and categorised in terms of the inter-storey drifts (global lateral deformation). The limit inter-storey drifts considered were those suggested in ATC 40, table 11-2. More specifically, Damaged Control level limits were a maximum total drift (θ) lying in the 0.01–0.02 radians interval and maximum inelastic drift (θ_{inelas}) in the 0.005–0.015 rad interval, whereas for Immediate Occupancy the limit values were of 0.01 and 0.005 in the same order.

These results confirm that the structure meets the Damage Control level, since interstorey drift angles never exceed 0.02 rad. However, the second and third storeys drifts have very low peak values and for that reason meet the Immediate Occupancy performance level.

However, the residual plastic deformation values, expressed by the drift θ at the end of the loading period, lie within the Damage Control range as well. Therefore, the overall structural performance only meets the Damage Control level, since structural performance is mainly conditioned by the behaviour of the first storey.

The results of the dynamic analysis performed on the analytical model of the retrofitted structure are presented in Table 7 and Fig. 10. They show that the deformations in the second and third storeys have decreased while the deformations of first storey have

Table 6
New relative displacements heights, total and inelastic drifts angles at each storey.

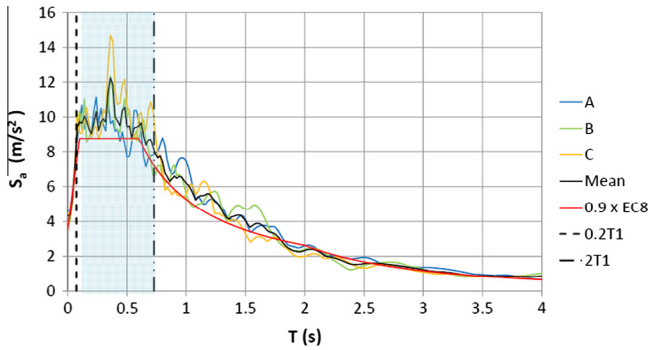| Storey	d_r (m)	h (m)	θ (rad)	$θ_{inel}$ (rad)
1	0.038	3.6	0.0106	0.0088
2	0.039	3.5	0.0112	0.0094
3	0.045	3.5	0.0128	0.00109

Fig. 8. Response spectra for accelerograms A, B and C, mean accelerogram and EC8 response spectrum reduced to 90%.
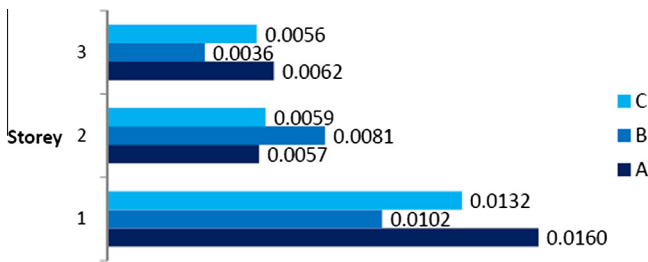
Fig. 9. Peak interstorey drifts resulting from each accelerogram (rad).

Table 7
Peak interstorey displacement resulting from each accelerogram.
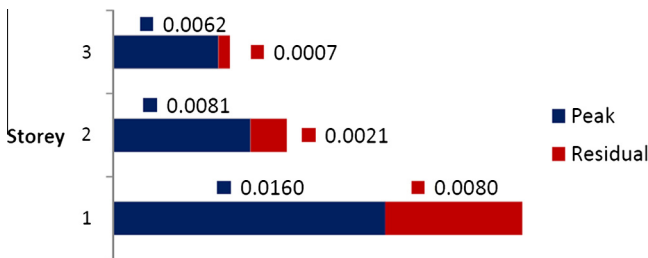
Accelerogram	Δ (cm)
A	8.5
B	7.4
C	6.6

Fig. 10. Peak and residual interstorey drift angles at each storey (rad).

tion of the overshoot factor. Furthermore, the increase in inertia forces associated with the first storey, following the yielding of the BRBs, is compounded by cyclic degradation model considered for RC elements under transient loading. In this case, the importance of the cyclic degradation model is more significant, given the lengthy duration of the accelerograms.

Nonetheless, the observed overall structural performance was still satisfactory and within expectations. The observation that the results vary according to the accelerogram and the RC cross-sections behaviour model, demonstrates how difficult it is to predict the response of an RC structure retrofitted with BRBs, when subjected to ground motion. However, these results also indicate that consideration of the overshoot factor could be a good design procedure when this type of device is used in structural retrofitting. Table 7 summarises the peak values of top storey displacement. These values are substantially lower than those obtained through the static pushover analysis (12.2 cm). This fact might be related to the cyclic degradation of the RC elements used in the dynamic analyses.

Analogously to the representation of top storey displacement, Table 8 shows the respective peak base shear values, which, in spite of scatter, are close to that obtained through pushover analysis.

7. Conclusions

The results of the analyses indicate that BRBs can be used as an effective way of increasing the seismic performance of RC structures, particularly existing structures that do not comply with current codes. However, the use of such devices is mostly restricted to steel framed structures. In fact, the existing standards for BRBs are mainly American or Japanese, and the design procedures described in them are mostly applicable to steel building structures. However, European standards still fail to provide any BRB design guidelines, despite mentioning passive control systems (BRBs in particular) as viable anti-seismic devices.

A simplified method for predicting the response of damped RC structures has been studied and employed in the preliminary design of a retrofitting scheme, using BRBs in a three-storey RC school building located in a high seismicity region of Portugal. Despite providing a significant increase in strength and capacity for sustaining lateral deformations, the results have indicated an important flaw in the method. After the early and almost simultaneous yielding of the dampers in all three storeys, lateral deformations were concentrated in the most flexible storey, which in this case is the first one, where columns were assumed to be pinned at their base. This resulted in excessively high ductility demands for the BRBs in the first storey and very small ductility demands for those in the upper storeys, which is a consequence of the clearly non-uniform distribution of interstorey drifts.

To overcome this flaw, an additional design step is proposed. This consisted of adopting an overshoot factor for the yield strength of the BRBs located in the most flexible storey. Based on a simple reasoning, a closed-form formula for this overshoot factor has been derived and presented. The implementation of the proposed overshoot factor modification was proven to attain the

increased, even with the use of the overshoot factor for the yield strength of first storey BRBs. This means that a significant concentration of deformation in the first storey still occurred. This may be because of the variation of inertia forces distribution, which was not considered either in static pushover analysis or in the formula-

Table 8
Peak base shear resulting from each accelerogram.

Accelerogram	F_b (kN)
A	4 804.8
B	4 089.5
C	4 554.4

required objective of uniform inter-storey drift distribution at performance point.

Using this overshoot factor led the subsequent pushover analysis to show significant improvement in the structural performance of the building under study, confirming the effectiveness of the overshoot factor concept.

Afterwards, nonlinear dynamic analysis confirmed that the strengthened structure met the Damage Control level, however strongly conditioned by the behaviour of first storey columns. These columns were modelled as pinned at their base because of the very limited strength of the foundations. Regarding residual plastic deformations, the values given by the three accelerograms were within the range of Damage Control deformations as well. These values might possibly have been lower if the ductility considered in the design of BRBs had been lower too, although at the expense of a potential decrease of energy dissipation. However, reducing residual plastic deformations by decreasing BRB ductility demand is only a possibility.

The use of the overshoot factor modification in the design of the ground storey BRBs led to a more uniform distribution of ductility demands in the BRBs along the height of the building and thus, to a more linear interstorey drift, therefore postponing the soft storey formation at the ground storey. In fact, the most important benefit of this design modification is the possibility of compensating the uneven distribution of either stiffness or strength along the height of the building by establishing adequate BRB yielding values for each storey.

The variability of the results from the different nonlinear analyses (Static and Dynamic) might be explained by the variability of the employed accelerograms (and long duration), by the complexity in modelling the material cyclic behaviour and also by an overly conservative estimate of the hysteretic damping ratio in the pushover analysis. All these problems demonstrate how difficult it is to predict seismic structural responses in the nonlinear range and the difficulty in the design of ideal damping systems.

References

[1] CT115(LNEC). NP EN 1998-1 Norma Portuguesa Eurocódigo 8: Projecto de estruturas para a resistência aos sismos-Parte1: Regras gerais, acções sismicas e regras para edifícios. Lisboa: IPQ; 2010.

[2] Kasai K, Kibayashi M. Manual for buildings passive control technology Part-1 manual contents and design/analysis methods. In: 13th world conference on earthquake engineering, Vancouver, BC, Canada; 2004.

[3] Kasai K. Current status of Japanese passive control scheme for mitigating seismic damage to buildings and equipments. In: First international conference on urban earthquake engineering. Japan: Center for Urban Earthquake Engineering, Tokyo Institute of Technology; 2004.

[4] FEMA. FEMA 450-1 – NEHRP recommended provisions for seismic regulations for new buildings and other structures – Part 1: provisions. Washington: Building Safety Council of the National Institute of Building Sciences, Federal Emergency Management Agency; 2003.

[5] AISC. Seismic provisions for structural steel buildings. AISC Seismic 2002.

[6] AISC. Seismic provisions for structural steel buildings. AISC Seismic 2005.

[7] NTC08. NTC'08: NTC Norme Tecniche per le Costruzioni, technical standards for construction. Gazzeta Ufficiale della Republica Italiana; 2008 [in Italian].

[8] OPCM. OPCM 3274/03 – Primi elementi in materia di criteri generali per la classificazione sismica del territorio nazionale e di normative techiche per la construzione in zona sismica. OPCM; 2003 [in Italian].

[9] OPCM. OPCM 3431/05 – Ulteriore modifiche ed integrazioni all'OPCM 20 marzo 2003 n. 3274, recante«Primi elementi in materia di criteri generali per la classificazione sismica del territorio nazionale e di normative techiche per la construzione in zona sismica. OPCM; 2005 [in Italian].

[10] CEN. EN15129 – anti-seismic devices. Brussels: Comité Européen de Normalisation; 2009.

[11] Kasai K, Fu Y, Watanabe A. Passive control systems for seismic damage mitigation. J Struct Eng 1998;124:501–12.

[12] Castellano M, Cappanera F, Balducci F, Antonucci R. Strutture prefabbricate con controventi dissipativi: l'esempio del nuovo polo didattico della Facoltá di Ingegnaria dell'Università Politecnica delle Marche di Ancona. Fip Industriale report, Padova, Italy; 2006 [in Italian].

[13] Kasai K, Hito H. Manual for building passive control technology Part 8-peak response evaluation and design for elasto-plastically damped system. In: 13th world conference on earthquake engineering, Vancouver B.C., Canada; 2004.

[14] Seimosoft. Seismostruct – a computer program for static and dynamic non linear analysis of framed structures. Available: <www.seismosoft.com>.

[15] Mander J, Priestley M, Park R. Theoretical stress-strain model for confined concrete. J Struct Eng 1988;114(8):1804–26.

[16] Martinez-Rueda J, Elnashai A. Confined concrete model under cyclic load. J Mater Struct 1997;30:139–47.

[17] Menegotto M, Pinto P. Method of analysis for cyclically loaded reinforced concrete plane frames including changes in geometry and non-elastic behaviour of elements combined normal force and bending. Symposium on the resistance and ultimate deformability of structures acted on by well defined repeated loads. Zurich, Switzerland: International Association for Bridge and Structural Engineering; 1973. p. 15–22.

[18] Filippou F, Popov E, Bertero V. Effects of bond deterioration on hysteretic behaviour of reinforced concrete joints. College of Engineering of the University of California. Report EERC-83-19. Berkeley: Earthquake Engineering Research, University of California; 1983.

[19] Monti G, Nuti C. Non-linear cyclic behaviour of reinforcing bars including buckling. J Struct Eng ASCE 1992;118:3268–84.

[20] Fragiadakis M, Pinho R, Antoniou S. Modelling inelastic buckling of reinforcing bars under earthquake loading. In: Progress in computational dynamics and earthquake engineering. A.A. Balkema Publishers – Taylor & Francis; 2008. p. 363–77.

[21] Prota A, De Cicco F, Cosenza E. Cyclic behaviour of smooth steel reinforcing bars: experimental analysis and modelling issues. J Earthquake Eng 2009;13:500–19.

[22] Council AT. ATC 40-seismic evaluation and retrofit of concrete buildings, vol. 1. State of California: California Seismic Safety Commission; 1996.

[23] CEN. EN 1998-1 Eurocode 8: design of structures for earthquake resistance – Part 1: general rules, seismic action and rules for buildings. Brussels: Comité Europeén de Normalisation; 2004.